Journal of Thermal Analysis and Calorimetry (2023) 148:13349–13362
https://doi.org/10.1007/s10973-023-12655-7

Thermal properties and the decomposition path of novel UV polymers of terpene-based monomer: citronellyl methacrylate

Katsiaryna Makowskaya[1] · Patrycja Jargieło[1] · Marta Worzakowska[1] · Magdalena Rogulska[1]

Received: 24 April 2023 / Accepted: 4 October 2023 / Published online: 18 November 2023

Abstract

Thermal properties and the decomposition path of more environmentally friendly polymers in both atmospheres: inert and oxidizing have been studied with a use of simultaneous TG/FTIR/QMS and DSC methods. The polymeric materials in the UV-polymerization process of cyclohexyl methacrylate and methacrylate monomer obtained from natural terpene alcohol: citronellol, using different compositions of monomers were prepared. The glass transition temperature (T_g) and thermal stability of these high solvent and chemical resistant materials were dependent on the composition and increased with increasing cyclic monomer content in the compositions. The T_g changed from 9.8˚C to 47.5˚C and a thermal stability from 195˚C to 222˚C (inert atmosphere) and from 160˚C to 217˚C (oxidizing atmosphere). The TG/FTIR/QMS analysis proved the emission of cyclohexyl methacrylate, citronellyl methacrylate and their lower molecular mass decomposition fragments, e.g., propene, cyclohexane, citronellol, citronellal, formic acid, methacrylic acid and CO, CO_2 during heating of these materials in helium and air atmospheres. It indicated the same radical mechanism of their decomposition in both atmospheres which meant that the presence of oxygen did not affect the course of decomposition but reduced the initial decomposition temperature of the copolymers.

Keywords Copolymers · Citronellyl methacrylate · Cyclohexyl methacrylate · DSC · TG/FTIR/QMS

Introduction

Recently, the intensive research is underway to synthesize new polymer materials that will be more environmentally friendly compared to petrochemical polymers and will have better or completely different properties compared to commercially available polymers. We can distinguish two basic paths for obtaining new polymeric materials, such as the modification of already existing polymers or the synthesis of polymers based on new monomers. In the case of the first of them, natural polymer materials such as starch, cellulose, chitosan, and rubber are subject to various modification processes in order to obtain biodegradable materials with improved properties compared to the starting material. Such modified polymer materials are used in many industrial sectors, for example, in the food, pharmaceutical, medical or chemical industry [1–6].

The second method, as mentioned above, is their synthesis on the basis of already known or new monomers. Among a wide range of polymers, this method is used to synthesize, among others, acrylic and methacrylic polymers [7–10]. The UV curable coatings obtained from acrylated epoxidized soybean oil and tannic acid-based hyperbranched methacrylates [11], nanohydrogels prepared from dextran and glycidyl methacrylate, 2-hydroxyethyl methacrylate and hydroxy-terminated HEMA-lactate [12], polymers from vanillin methacrylate [13, 14], polymers prepared with the use of guaiacol methacrylate or eugenol methacrylate [15, 16] are known and described in the literature. The preparation of bio-based meth(acrylates) from terpenes such as (+) α-pinene, (−) β-pinene, (+) (*R*)-limonene, and (−) (*R*)-carvone is also described. These bio-based meth(acrylates) are polymerized with a chain transfer agent (dodecanemercaptan) to get novel transparent materials [17–20]. The polymers from menthyl acrylate, sorbrerol acrylate, sorbrerol methacrylate and tetrahydrogeraniol acrylate are also known [21–23]. The polymerization of lactate-based

✉ Marta Worzakowska
marta.worzakowska@poczta.umcs.lublin.pl

[1] Department of Polymer Chemistry, Institute of Chemical Sciences, Faculty of Chemistry, Maria Curie-Skłodowska University, Gliniana 33 Street, 20-614 Lublin, Poland

acrylates allows obtaining the corresponding homopolymers with the glass transition temperatures depending on their composition and the thermal stability above 190 °C [24, 25]. Also, the bio-based acrylates from isosorbide are described [26–28]. The polymerization of solketal acrylate with styrene or *N*-isopropyl acrylamide leads to prepare the amphiphilic block copolymers [29, 30]. In turn, polymerization of solketal acrylate with methyl acrylate gives the self-assembling materials [31]. In turn, the copolymerization of solketal meth(acrylates) with various transfer agents such as 2-mercaptoethanol, dodecanethiol, and thiols based on lauric and oleic acids leads to water-soluble glycerin-based polymers [32]. The homopolymerization or copolymerization of bio-based acrylates from levoglucosenone allows preparing the new materials with promising thermal stability and a high glass transition temperature [33, 34]. By appropriate selection of co-monomer for copolymerization of meth(acrylates) prepared from vegetable oils and fatty acids, it is possible to prepare a whole range of polymeric materials with various unique properties [35–38]. The researches on obtaining new monomers based on natural compounds are still intensively conducted in order to synthesize the new polymer materials with unique properties for various applications.

The present paper focuses on the thermal properties and decomposition path of UV-polymerized, more environmentally friendly polymers obtained from two methacrylic monomers, i.e., cyclic monomer (cyclohexyl methacrylate) and methacrylic monomer derived from natural terpene alcohol: citronellol. The influence of the structure of polymers and their composition on the glass transition temperature, thermal resistance and decomposition path in inert and oxidizing atmospheres was evaluated.

Experimental

Materials and method

Citronellyl methacrylate was prepared according to the method presented in these references [39–41]. Cyclohexyl methacrylate was from Sigma-Aldrich. Irgacure 651 (2,2,-dimethoxy-1,2-diphenylethan-1-one), methanol, butanol, acetone, acetic acid, ethyl acetate, tetrahydrofurane, diethyl ether, dioxane, chloroform, CCl_4, hexane, cyclohexane, toluene and silica gel were from Merck. Sodium hydroxide, carbon tetrachloride, hydrochloric acid and buffers solutions (pH 4, 7, 10) were delivered by POCh, Gliwice, Poland.

UV-polymerization

The prepared compositions, Table 1, were irradiated by a use of a TL20W/05 SLV low pressure mercury lamp (340–365 nm). The circle samples (30 mm diameter and 1 mm thickness) were irradiated for 15 min at 25ºC to obtain foils. After UV polymerization, the foils were placed in the dryer at 50 ºC for 2 h and at 120 ºC for 1 h to complete the polymerization process.

Characterization of the copolymers

The structures of the prepared polymers by the use of the FTIR Tensor 27 instrument (Bruker, Germany) were investigated. The FTIR spectra (KBr tablets) from 600 cm^{-1} to 4000 cm^{-1} with 4 cm^{-1} resolution and 62 scans per spectrum were collected.

In addition, based on the FTIR spectra, the conversion degrees of the C = C bonds (*DC*) were evaluated. The *DC* values were estimated by the comparison of the C = C bands area at 1635–1637 cm^{-1} (methacrylic bonds) and at 1674 cm^{-1} (ethylenic bonds) with the C = O band area at 1720 cm^{-1}. The following equation was applied:

$$DC/\% = 100 \times \left[1 - \left(R_{polymer}/R_{monomer}\right)\right]$$

where *R*—the surface area of the C = C band/surface area of the C = O band.

The cross-polarization magic angle spinning (^{13}C CPMAS/NMR) spectra by the use of a Bruker Avance 300 MSL instrument (Bruker, Germany) were collected. The

Table 1 The UV compositions

Polymeric material	Citronellyl methacrylate (CitM)/g	Cyclohexyl methacrylate (CM)/g	Irgacure 651/g	Mass ratio of monomers (CitM: CM)/ %
Copolymer 1	0.6	2.4	0.09	20:80
Copolymer 2	1.5	1.5	0.09	50:50
Copolymer 3	2.4	0.6	0.09	80:20
PCitM	3.0	–	0.09	100:0
PCM	–	3.0	0.09	0:100

where PCitM – poly(citronellyl methacrylate), PCM – poly(cyclohexyl methacrylate)

resonance frequency 75.5 MHz, the number of scans 2048 and the spin rate 7300 Hz were applied.

The gravimetric method in order to evaluate the solubility of the polymers in the solvents of different polarity was used. The samples (mass ca. 0.2 g) in the chosen solvents were placed. For the first week of testing, each sample was taken out from the solvent, drained and weighed daily. Then, the samples were weighed once a weak and once a month. The solubility study took a total of 6 months. The mass change (ΔmS, %) of the material was determined according to:

$$\Delta mS = (m_1 - m_2)/m_1 \times 100\%$$

m_1—the initial polymer mass, m_2—the final polymer mass, ΔmS—the mass change (a solubility).

The chemical resistance of the polymers in 1 M NaOH, buffer solutions with pH 4, 7 and 10 and 1 M HCl was studied. The samples (mass ca. 0.2 g) in chosen solutions were placed. The samples in the same manner as the samples in the solubility tests were weighed. The chemical resistance study took a total of 6 months. The mass change (ΔmR, %) was counted based on the equation [42]:

$$\Delta mR = (m_1 - m_2)/m_1 \times 100\%$$

m_1—the initial polymer mass, m_2—the final polymer mass, ΔmR—the mass change (a chemical resistance).

The glass transition temperatures (T_g) of the prepared polymers with the use of a DSC method were evaluated. The samples (mass ca. 10 mg) in Al crucible with a pierced lid between minus 120 °C and 150 °C were heated, cooled down to minus 120 °C and then reheated to 150 °C. An argon with a flow rate 40 mL min^{-1} as a furnace atmosphere was applied. The heating rate was 10 K min^{-1}. The T_g values from the second DSC scan were determined.

The thermal stabilities of the prepared polymers with a use of the TG/DTG method (a STA 449 Jupiter F1 apparatus, Netzsch, Germany) were evaluated. The samples (mass ca. 10 mg) in an open Al_2O_3 crucible were heated between 40 °C and 550 °C with a heating rate 10 K min^{-1}. These researches in helium (a flow rate 40 mL min^{-1}) and in a synthetic air (a flow rate 100 mL min^{-1}) were made. The temperature where there is 5% of mass loss ($T_{5\%}$), DTG maximum temperatures (T_{max}), mass losses (Δm) and residual masses (rm) were determined.

The pyrolysis and oxidative decomposition paths of the novel polymeric materials based on the type of gases emitted during heating were specified with the use of a STA 449 Jupiter F1 apparatus (Netzsch, Germany) coupled on-line with a FTIR (FTIR TGA 585, Bruker, Germany) and a QMS (QMS 403 C Aëolos, Germany) analyzers. The FTIR TGA 585 with a Teflon tube (a diameter of 2 mm) heated to 200 °C was connected on-line to a STA. The FTIR spectra in the range of 600–4000 cm^{-1} with 4 cm^{-1} resolution were gathered. In turn, the QMS 403 C Aëolos with a quartz capillary heated to 300 °C was connected on-line to a STA. The QMS electron ionization was 70 eV. The QMS spectra in the range of 10–170 m/z were collected.

Results and discussion

Characterization of the structure

The FTIR spectra for the prepared polymers are shown in Fig. S1 in Supplementary file. The simplified diagram of the polymer's structure is presented in Scheme S1 in Supplementary file. As it is well visible, citronellyl methacrylate monomer has two types of the double bonds: methacrylic bond and ethylenic bond. In turn, cyclohexyl methacrylate has a one type of the double bond: methacrylic bond. In the used experimental conditions, the polymerization of these two types of the double bonds is expected. The characteristic, stretching methacrylic double bonds vibrations at 1635–1637 cm^{-1} are located. The stretching ethylenic double bonds vibrations at 1674 cm^{-1} are visible [39, 43]. Fig. S1 shows only residual intensities of previously mentioned vibrations. The *DC* values calculated based on the FTIR spectra, after conditioning the samples at 120 °C, are in the range 94–96%, Table 2. The FTIR results and the calculated *DC* values confirm that methacrylic and ethylenic double bonds take part in the UV polymerization and

Table 2 The conversion degrees of the C = C bonds (*DC*)

Polymeric material	*DC*/%									
	Irradiation time/min								Conditioning temperature/°C	
	1	2	3	4	5	10	13	15	50 °C	120 °C
Copolymer 1	54	67	72	73	75	77	78	84	88	95
Copolymer 2	64	73	76	78	79	80	82	83	87	96
Copolymer 3	60	70	74	75	77	79	80	81	85	94
PCitM	51	59	60	61	62	65	67	68	80	90
PCM	50	57	59	60	61	62	65	66	72	80

cross-linking. This leads to the formation of three-dimensional spatial networks, Scheme S1 [44–47].

Table S1 (Supplementary file) shows the characteristic chemical shifts in the ^{13}C CP/MAS NMR for the prepared polymers. The carbonyl peaks in the unreacted methacrylic groups (165–166 ppm) for copolymers 1–3 are present on the NMR spectra, but their intensity is very low. The carbonyl peaks in the reacted methacrylic groups are visible very well (175–176 ppm) in a spectrum. Moreover, carbons with unreacted ethylenic bonds with a low intensity are also observed (125 and 135 ppm). The % of the reacted double bonds on the basis of NMR spectra was calculated. The NMR calculated % of the reacted double bonds is comparable with these values evaluated from the FTIR. It is 94% for copolymers 1 and 2 and 92% for copolymer 3. These results additionally confirm a high conversion of the double bonds during the UV polymerization and stabilization of the tested copolymers.

Solvent and chemical resistance

Tables 3 and 4 show the solubility results. The copolymers and PCitM are characterized by a very low solubility in polar and non-polar solvents. Their solubility is below 1%. In turn, PCM homopolymer is a soluble material in the solvents such as toluene, chloroform, dioxane, CCl_4, acetone, acetic acid and tetrahydrofurane. Its solubility in these solvents is due to its chemical structure and linear chain structure without crosslinks. However, the insolubility of the copolymers and PCitM is connected with its branched structure containing additional crosslinks as it is proved from the FTIR and ^{13}C CP/MAS NMR analyses.

When we look at the chemical resistance results, Table 5, we can see a similar trend as for the solubility results. The obtained copolymers and PCitM are the materials with a high resistance to acidic, basic and buffer solution environments. The mass loss is below 0.5%. These studies proved high chemical and solvent resistance of the prepared materials, due to their cross-linked structures. Such materials can be an attractive for the production of elements working in contact with solvents and various chemical environments [48, 49].

Table 3 The mass change (ΔmS, %) in polar solvents

Polymer name	ΔmS/%						
	Water	Methanol	Butanol	Acetone	Acetic acid	Ethyl acetate	Tetrahydro-furan
Copolymer 1	0.4	0.5	0.7	0.9	1.0	0.8	0.5
Copolymer 2	0.5	0.6	0.7	0.9	1.0	0.7	0.6
Copolymer 3	0.4	0.5	0.6	0.7	0.9	0.7	0.6
PCitM	0.4	0.3	0.3	0.5	0.9	0.7	0.6
PCM	0.8	1.5	1.2	Soluble	Soluble	2.5	Soluble

Table 4 The mass change (ΔmS, %) in non-polar solvents

Polymer name	ΔmS/%						
	Diethyl ether	Dioxane	Chloroform	CCl_4	Hexane	Cyclo-hexane	Toluene
Copolymer 1	0.5	0.9	0.9	0.7	0.8	0.7	0.9
Copolymer 2	0.5	0.8	0.8	0.7	0.8	0.6	0.8
Copolymer 3	0.4	0.8	0.7	0.6	0.8	0.6	0.8
PCitM	0.3	0.9	0.6	0.6	0.8	0.6	0.7
PCM	0.7	Soluble	Soluble	Soluble	0.8	2.4	Soluble

Table 5 The mass change (ΔmR, %) in different environments

Polymer name	ΔmR/%				
	1 M NaOH	1 M HCl	Buffer pH = 4	Buffer pH = 7	Buffer pH = 10
Copolymer 1	0.5	0.3	0.3	0.4	0.4
Copolymer 2	0.5	0.3	0.3	0.3	0.5
Copolymer 3	0.4	0.2	0.2	0.3	0.4
PCitM	0.4	0.0	0.0	0.1	0.1
PCM	15.4	2.8	2.1	1.9	12.6

Glass transition temperature (T_g)

The DSC studies confirm that the glass transition temperature of the prepared polymers is directly depended on their composition. T_g value for the obtained PCM homopolymer is 65.9 °C. However, the PCitM homopolymer is characterized by a much lower T_g (3.1 °C). The T_g decreases from 47.5 to 9.8 °C with increasing citronellyl methacrylate content in the composition. It means that the copolymers containing a greater amount of citronellyl methacrylate are more flexible and softer. The presence of aliphatic segments (-CH_2-) originating from citronellyl methacrylate in the main and side chains in the created polymer network significantly increases its mobility at lower temperatures. Moreover, all the copolymers show only one T_g value, Fig. 1. This indicates that they are not mixtures of two homopolymers (blends). They are rather random copolymers.

Thermal properties (TG/DTG) in helium

Figure 2 shows the TG/DTG curves for the prepared polymers in helium atmosphere. In Table 6, the TG/DTG data are collected. The thermal resistance marked as the temperature where there is a mass loss of 5% ($T_{5\%}$) is directly depended on the composition of the copolymers. The thermal resistance of the materials decreases with increasing citronellyl methacrylate content in the compositions. The copolymer 1, derived from 20 mass% of citronellyl methacrylate and 80 mass% of cyclohexyl methacrylate, is characterized by the highest thermal resistance (222 °C). Its thermal stability is even higher than that of PCM (215 °C). However, the copolymer 3 (80 mass% of citronellyl methacrylate and 20 mass% of cyclohexyl methacrylate) has the lowest thermal resistance (195 °C), but its thermal stability is much higher than for PCitM (153 °C).

The thermal decomposition of the tested polymers happens in more than two main stages composed of at least two steps. In the case of copolymers 1–3, the first decomposition stage consists of at least two steps visible as the DTG maximum at 214–241 °C (T_{max1}) and at 351–358 °C

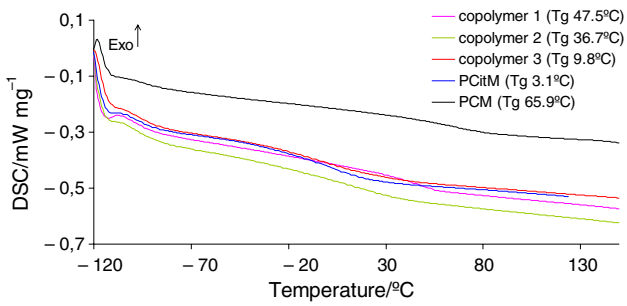

Fig. 1 The DSC curves for the prepared polymers

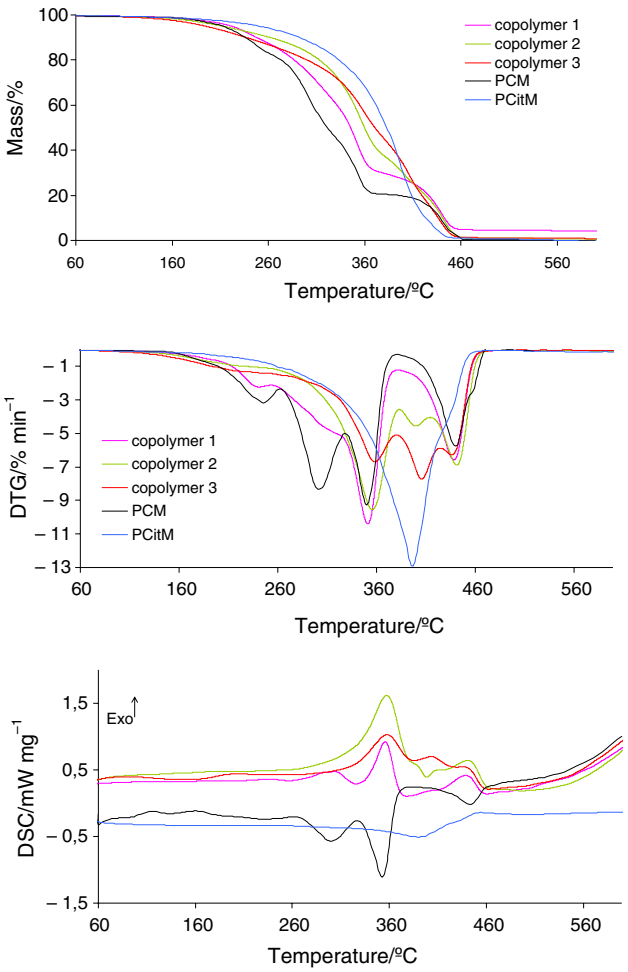

Fig. 2 The TG-DTG-DSC curves for the tested materials (helium atmosphere)

(T_{max1a}). According to the TG results, the mass loss (Δm_1) is from 70.4% for copolymer 1 to 55.2% for copolymer 3 in this decomposition stage. The Δm_1 values are directly dependent on the composition of copolymers. They decrease as the content of citronellyl methacrylate in the copolymer increases. The second decomposition stage is appeared as one or two, non-well divided DTG signals at 399–406 °C (T_{max2}) and at 436–441 °C (T_{max2a}). The mass loss (Δm_2) is from 25.7% (copolymer 1) to 44.4% (copolymer 3), and it also depends on the composition. However, the decomposition process of the PCitM homopolymer includes two basic stages. The first at T_{max1} 252 °C with the mass loss 28.7% is characterized by a low-intensity DTG signal. The second one happens above 300 °C with T_{max2} at 407 °C and with the mass loss 71.3%. In turn, the PCM homopolymer also decomposes in at least two main stages. The first one consists of at least three steps visible as the DTG maxima at 246, 302 and 351 °C. The mass loss

Table 6 The TG-DTG data for the tested materials (helium atmosphere)

Polymer name	$T_{5\%}$ /°C	T_{max1}/T_{max1a} /°C	Δm_1 /%	T_{max2}/T_{max2a} /°C	Δm_2 /%	rm /%
Copolymer 1	222	241/351	70.4	438	25.7	3.9
Copolymer 2	213	214/356	63.4	399/441	36.6	0
Copolymer 3	195	214/358	55.2	406/436	44.4	0.4
PCitM*	251	396	99.2	577	0.8	0
PCM	213	246/302/351	79.6	440	20.4	0

* As cited in Ref [50]

is 79.6%. The second one spreads above the temperatures 400 °C with T_{max2} at 440 °C and the mass loss 20.4%.

An interesting relationship is noticed between the DSC curves and TG/DSC curves, Fig. 2. The decomposition process of the PCitM and PCM homopolymers is described only by the endothermic DSC signals. It indicates the cleavage of the suitable bonds (pyrolysis) in the structure of this homopolymers during the heating. However, mainly the exothermic DSC signals for the tested copolymers are observed. This may be due to the interactions of the created intermediate volatiles under the pyrolysis of the tested materials. Thus, some chemical reactions between the volatiles are expected. This is the confirmation that the pyrolysis of the copolymers proceeds in a different way and is more complicated as compared to the decomposition process of homopolymers.

Simultaneous TG/DTG/FTIR/QMS—decomposition course in helium.

Figure 3 presents the gaseous 3D FTIR spectra and the 2D FTIR spectra extracted for the characteristic temperatures. As one can see, the mixture of volatiles is emitted. This is confirmed by the presence of the absorption bands at different wavelengths. The beginning of the emission of some decomposition gaseous products at $T_{5\%}$ is noticed. The volatile emission increases as the heating temperature increases which is observed as an increase in the intensity of the FTIR signals. Between the temperatures $T_{5\%}$ and T_{max1a}, the following absorption signals: above 3500 cm^{-1} (the OH stretching vibrations), at 3037–3014 cm^{-1} (the = C-H stretching vibrations), in the range of 2962–2861 cm^{-1} (the C-H stretching vibrations), at 2358–2333 cm^{-1} (CO_2), at 1714 cm^{-1} (T_{max1}) and at 1756–1731 cm^{-1} (T_{max1a}) (the C = O stretching vibrations), at 1670–1636 cm^{-1} (the C = C stretching vibrations), at 1492–1550 cm^{-1} (the C-H vibrations of cyclohexane ring), at 1457–1446 cm^{-1} and at 1388–1376 cm^{-1} (the C-H deformation vibrations), at 1305–1118 cm^{-1} (the C-O stretching vibrations), and the bands from 1027 to 650 cm^{-1} (the = C-H out of plane deformation vibrations) are indicated.

At T_{max2}, the same absorption bands as at T_{max1a} are observed. However, its intensity is low. In addition, the shift in the wavenumber of absorption bands for the C = O stretching vibrations (1776–1741 cm^{-1}) is visible. Also, at the second decomposition stage, the creation of CO (2156–2088 cm^{-1}) and the increase in the emission of CO_2 (2358–2333 cm^{-1}) are well indicated [51–58].

To analyze well the type of the volatiles, the gaseous QMS spectra were also collected at different temperatures. The QMS spectra prove the formation of the various *m/z* ions whose values depend on the temperature, Fig. 4. Analyzing the QMS spectra at the beginning of the decomposition ($T_{5\%}$), the *m/z* ions with the following values: 14, 15, 16, 17, 18, 27, 28, 29, 32, 36, 39, 40, 41, 54, 55, 67, 69, 81, 82, 83, 97 are clearly observed. As the temperature increases above $T_{5\%,}$ the intensity of the *m/z* ions also increases. At T_{max1}, the same *m/z* ions as at $T_{5\%}$ are visible, and however, their intensity is greater. In turn, at T_{max1a}, the intensities of *m/z* ions are maximum. At T_{max1a}, the *m/z* ions: 14, 15, 16, 17, 18, 26, 27, 28, 29, 31, 32, 36, 37, 38, 39, 40, 41, 42, 43, 44, 50, 51, 52, 53, 54, 55, 56, 57, 63, 65, 66, 67, 68, 69, 77, 78, 79, 81, 82, 83, 87, 95 are appeared. Comparing the FTIR spectrum with the QMS spectrum collected at a specific temperature, one of the decomposition products is water: *m/z* 16 (O^+), 17 (HO^+), 18 (H_2O^+) and CO_2 (*m/z* 44 (CO_2^+), 28 (CO^+)). Cyclohexyl methacrylate or their decomposition products also to be expected as the degradation products. The QMS database confirms that during the ionization of cyclohexyl methacrylate, the *m/z* ions: 69 ($C_4H_5O^+$), 82 ($C_6H_{10}^+$), 41 ($C_3H_5^+$), 67 ($C_4H_5^+O$), 55 ($C_4H_7^+$), 54 ($C_4H_6^+$), 39 ($C_3H_3^+$), 83 ($C_6H_{11}^+$), 81 ($C_6H_9^+$) are formed [59]. These *m/z* ions are also visible on the experimental QMS spectra. However, the formation of the decomposition products of cyclohexyl methacrylate such as 1-propene (*m/z* 41 ($C_3H_5^+$), 39 ($C_3H_3^+$), 42 ($C_3H_6^+$), 27 ($C_2H_3^+$), 40 ($C_3H_4^+$), 38 ($C_3H_2^+$), 37 (C_3H^+), 26 ($C_2H_2^+$), 15 (CH_3^+), 14 (CH_2^+)), cyclohexane (*m/z* 56 ($C_4H_8^+$), 84 ($C_6H_{12}^+$), 41 ($C_3H_5^+$), 55 ($C_4H_7^+$), 69 ($C_5H_9^+$), 39 ($C_3H_3^+$), 42 ($C_3H_6^+$), 27 ($C_2H_3^+$), 43 ($C_3H_7^+$), 54 ($C_4H_6^+$)) and formic acid (*m/z* 29 (CHO^+), 46 ($CH_2O_2^+$), 45 (CHO_2^+), 28 (CO^+), 17 (OH^+), 44 (CO_2^+), 16 (O^+), 12 (C^+), 13 (CH^+), 30 (CH_2O^+)) are also expected and confirmed based on the experimental QMS spectra.

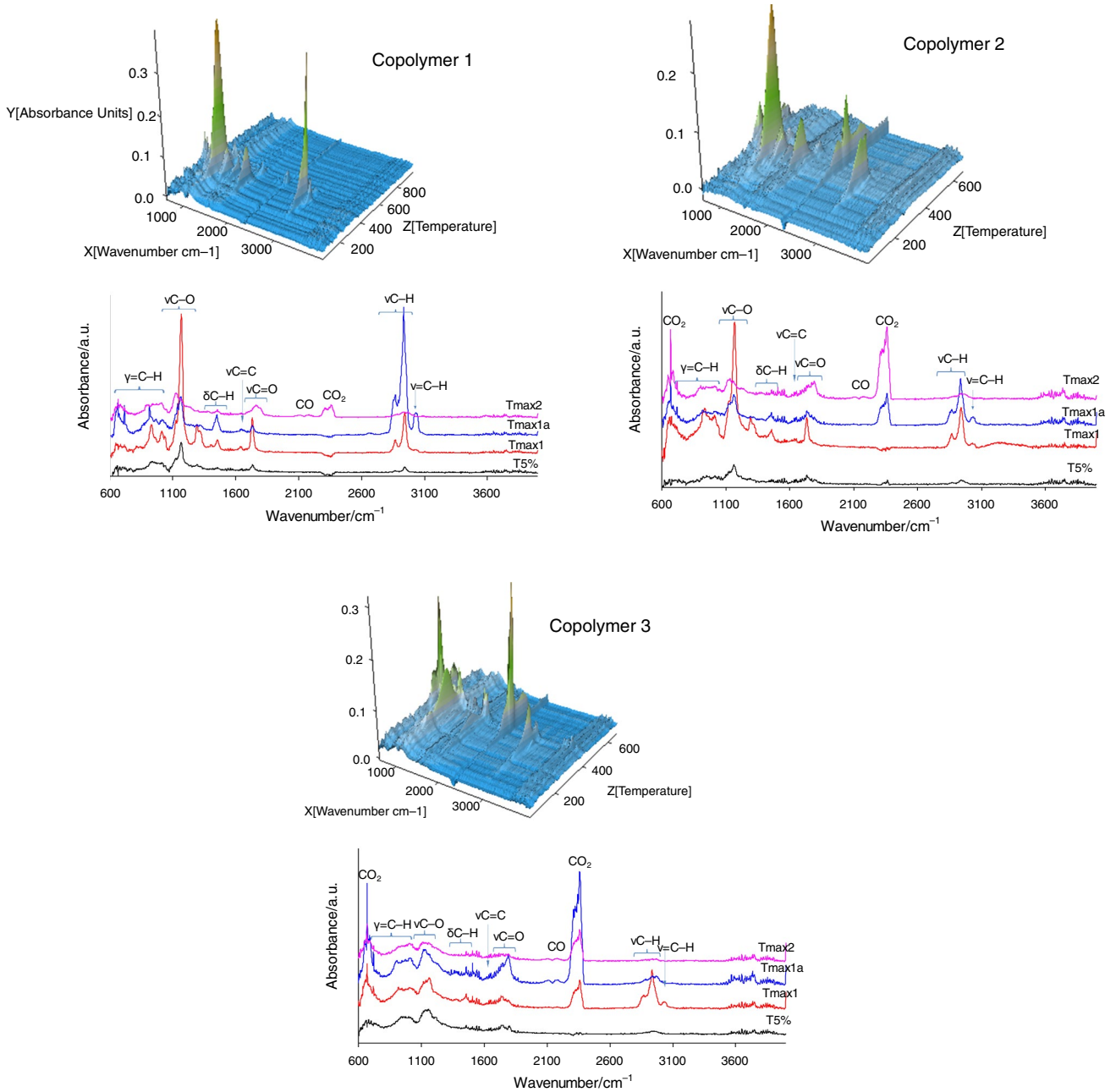

Fig. 3 The 3D FTIR spectra and the extracted FTIR spectra of the emitted volatiles for copolymers in helium

In our previous work, it was confirmed that the decomposition of poly(citronellyl methacrylate) led to the formation of citronellyl methacrylate ester as a result of its depolymerization [50]. The presence of the *m/z* ions: 39 ($C_3H_3^+$), 41 ($C_3H_5^+$), 50 ($C_4H_2^+$), 51 ($C_4H_3^+$), 52 ($C_4H_4^+$), 53 ($C_4H_5^+$), 54 ($C_4H_6^+$), 55 ($C_4H_7^+$), 56 ($C_4H_8^+$), 65 ($C_5H_5^+$), 67 ($C_5H_7^+$, $C_4H_3^+O$), 68 ($C_5H_8^+$, $C_4H_4^+O$), 69 ($C_5H_9^+$, $C_4H_5^+O$), 70 ($C_5H_{10}^+$), 77 ($C_6O_5^+$), 79 ($C_6H_7^+$), 81 ($C_6H_9^+$), 82 ($C_6H_{10}^+$) on the QMS spectra confirms that citronellyl methacrylate ester is one of the main volatiles during heating of the copolymers. However, due to the occurrence of an exothermic DSC signals, it can be assumed that among the decomposition products the gases formed as a result of decomposition of citronellyl methacrylate with lower molecular mass are emitted. Among volatiles, the presence of citronellol (*m/z* 71 ($C_4H_7O^+$), 68 ($C_5H_8^+$), 41 ($C_3H_5^+$), 69 ($C_5H_9^+$), 43, 55 ($C_4H_7^+$), 81, 56, 57, 67 ($C_5H_7^+$)), citronellal (*m/z* 41 (C_2HO^+), 69 ($C_5H_9^+$), 55 ($C_3H_3^+O$), 43 ($C_2H_3O^+$), 56 ($C_3H_4O^+$), 67 ($C_5H_7^+$), 29 ($C_2H_5^+$), 39 ($C_3H_3^+$), 27 ($C_2H_3^+$)), methacrylic acid (*m/z* 41 ($C_3H_5^+$), 86 ($C_4H_6O_2^+$),

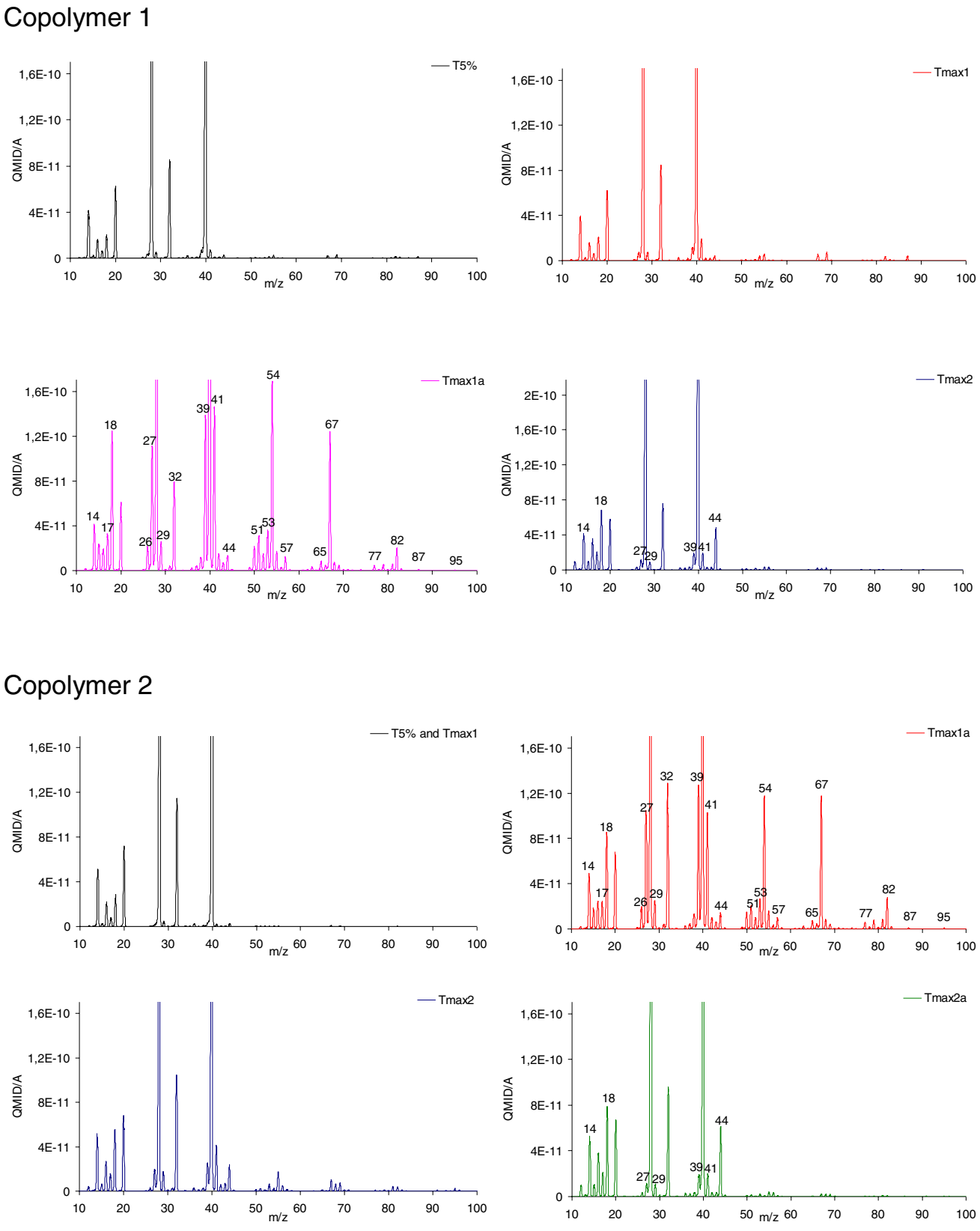

Fig. 4 The *m/z* ions of the emitted volatiles at the characteristic temperatures in helium

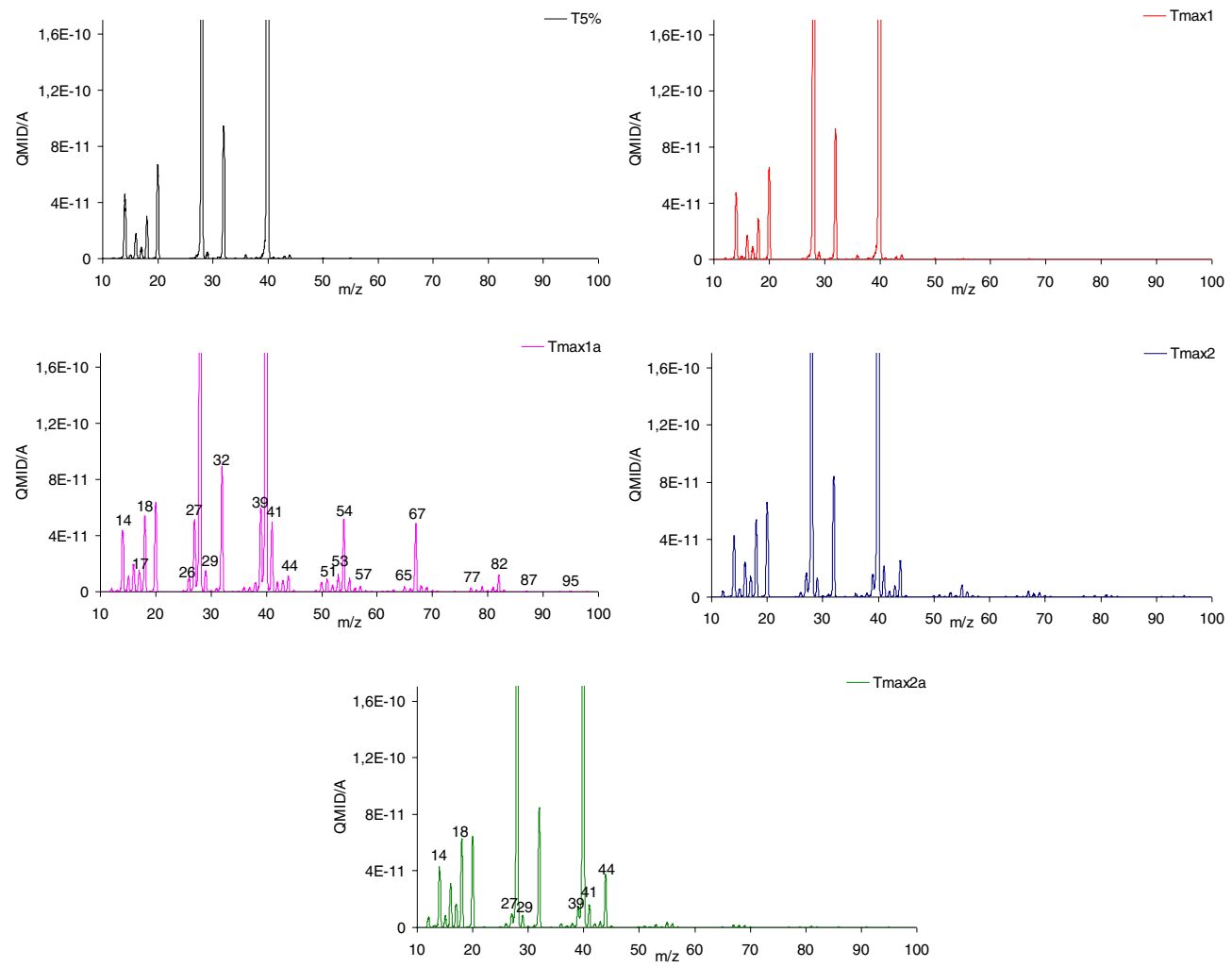

Fig. 4 (continued)

39 ($C_3H_3^+$), 40 ($C_3H_4^+$), 45 ($COOH^+$), 69 ($C_4H_5O^+$), 38 ($C_3H_2^+$), 68 ($C_4H_4O^+$), 37 (C_3H^+)), propene (41 ($C_3H_5^+$), 39 ($C_3H_3^+$), 42 ($C_3H_6^+$), 27 ($C_2H_3^+$), 40 ($C_3H_4^+$), 37 (C_3H^+), 26 ($C_2H_2^+$), 15 (CH_3^+), 14 (CH_2^+)) and its further decomposition, degradation and combination fragments are also expected [59].

Besides, the intensity of the FTIR absorption signals and QMS m/z ions changes depending on the composition of the copolymers. In the case of copolymer 2 which contains 80 mass% of cyclohexyl methacrylate, you can see the high intensity FTIR and QMS signals from poly(cyclohexyl methacrylate) fragments. In turn, for copolymer 3 which contains 80 mass% of citronellyl methacrylate, the FTIR and QMS signals with high intensity for the volatiles created from poly(citronellyl methacrylate) fragments are visible.

All the above results indicate that the pyrolysis of the tested polymers is complicated. It takes place in several stages involving pyrolysis processes, depolymerization, decarboxylation and further chemical reactions of intermediate products in a gaseous state. This leads to the emission of a gas mixture of different molar masses when the copolymers are heated in a helium atmosphere, Scheme 1.

Thermal properties (TG/DTG) in synthetic air

Figure 5 shows the TG/DTG curves for the tested polymeric materials under their heating in synthetic air conditions. The TG/DTG data are placed in Table 7. Based on the obtained data, it is well seen that the copolymer 2 which is composed of 50 mass% of citronellyl methacrylate and 50 mass% cyclohexyl methacrylate are

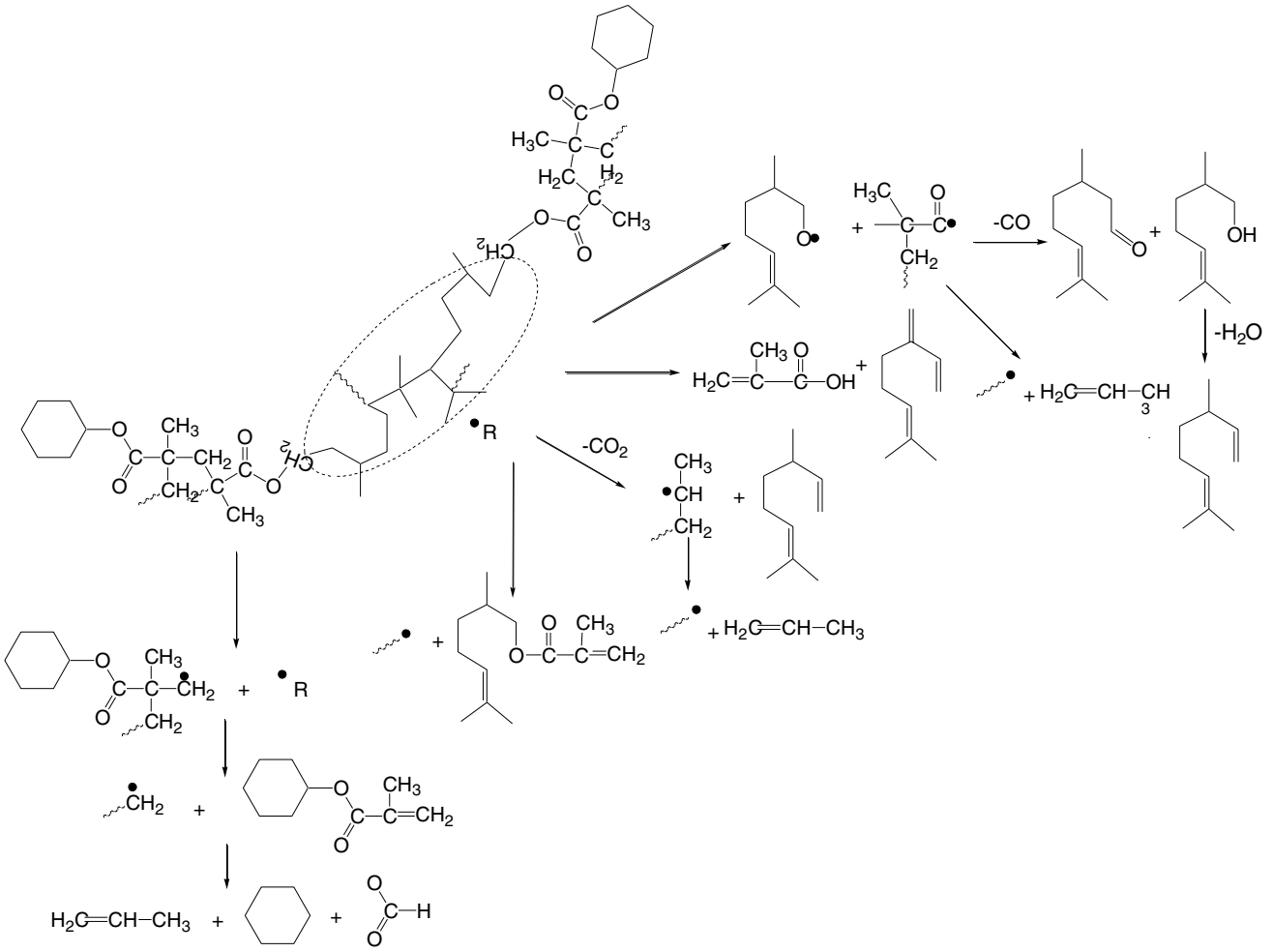

Scheme 1 The proposed decomposition path of copolymers in helium

characterized by the highest thermal resistance in air conditions (217 °C). The thermal stability of other tested copolymers is lower than 200 °C but higher than the thermal stability of poly(citronellyl methacrylate) homopolymer. Moreover, the thermal stability of the copolymers is lower in air atmosphere than in inert atmosphere. In addition, during the heating of the copolymers in air atmosphere, no effect of the content of methacrylate monomers on the increase or decrease the thermal stability is noticed. This is obviously due to the additional influence of oxygen and different effects of oxygen on the materials and possibility of various chemical reactions taking place between the materials and oxygen.

The tested copolymers decompose in at least three main stages. The first one spreads between $T_{5\%}$ and 373–380 °C with T_{max1} at 349–352 °C and with the highest mass loss from 60.7 to 67.8%. The second one is visible from ca. 373–380 °C to 445 °C with T_{max2} at 399–405 °C with the mass loss from 26.8 to 34.1%. In turn, the third one is from ca. 445 °C to 570 °C with T_{max3} at 496–508 °C and with the lowest mass loss (5.2–6.1%). The complete decomposition of copolymers in air conditions is observed.

Simultaneous TG/DTG/FTIR/QMS—decomposition course in synthetic air

Figure 6 shows the selected gaseous FTIR spectra extracted at the characteristic temperatures for copolymer 2. The FTIR spectra at $T_{5\%}$ and T_{max1} confirm the presence of the absorption bands originating from the stretching vibrations of the =C-H (3035 cm^{-1}), the C-H (2933–2860 cm^{-1}), the C=O (1782 and 1731 cm^{-1}), the C=C (1630 cm^{-1}), the C-O (1267–1022 cm^{-1}), the C-H deformation vibrations (1444 and 1357 cm^{-1}) and the =C-H out of plane deformation vibrations (1000–665 cm^{-1}). In turn, in the range of $T_{max2} - T_{max3}$ the FTIR bands for the stretching vibrations of the =C-H (3040 cm^{-1}), the C-H (2960–2870 cm^{-1}), the C=O (1781–1731 cm^{-1}), the C=C (1625 cm^{-1}), the C-O (1272–1022 cm^{-1}), the C-H deformation vibrations (1448 and 1376 cm^{-1}) and the =C-H out of plane deformation

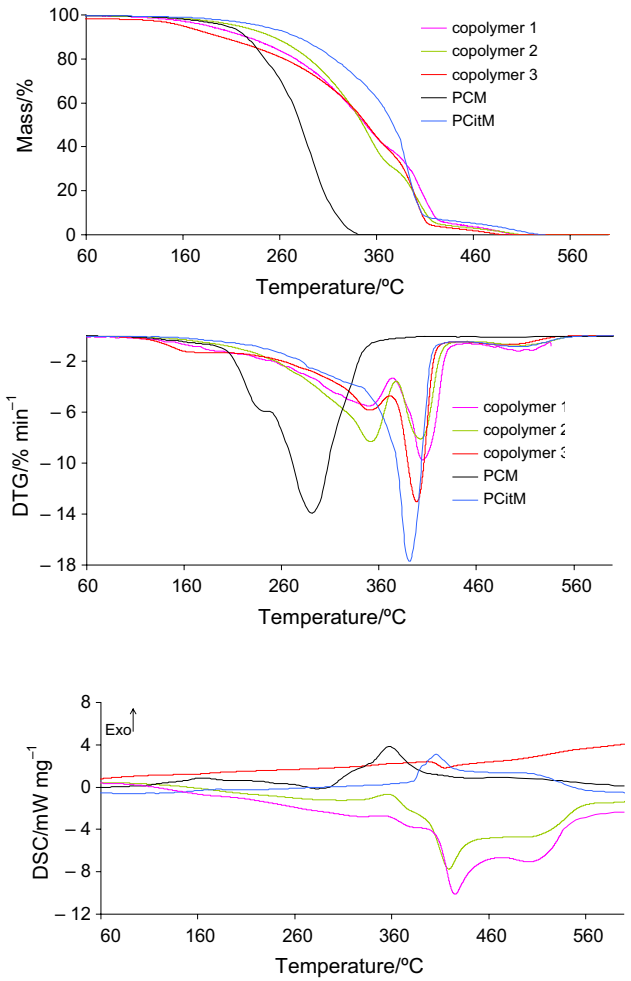

Fig. 5 The TG-DTG-DSC curves for the tested copolymers (synthetic air atmosphere)

vibrations (1000–885 cm^{-1}) are still present although they are somewhat shifted within the range of a different wavenumber. In addition, which is interesting in this temperature range, there is a little emission of CO_2 and CO. The emission of these gases is much lower compared to their emission in the atmosphere of helium. This situation is unexpected because usually in the presence of air atmosphere the chemical reactions including combustion and decarboxylation take place more easily. One of the exceptions is the inhibitory effect of oxygen on the polymerization reactions [60–62]. However, when we look closely at the DSC curves, it can be seen that the main processes during the heating of copolymers are endothermic processes, and therefore, they are related mainly to the breaking the bonds present in the structure of the polymer network. Only in T_{max1} a DSC exothermic peak of a slight intensity is observed, which may indicate some chemical reactions and thus the emission of CO_2 and CO at higher temperatures. It can be summarized that the presence of oxygen in the atmosphere allows the reduction of the activation energy of breaking the chemical bonds present in the structure of the obtained polymer network. This is evidence by lower initial decomposition temperatures of the copolymers compared to these temperatures in helium. In addition, these results also confirm the emission of such decomposition gases which, under the conditions of the conducted analysis, do not undergo or a slightly undergo chemical reactions with oxygen. Therefore, the TG/DSC/FTIR results prove that the main emitted volatiles are methacrylate esters. Next to them, the emission of acids (C=O at 1781 cm^{-1} and C-O at 1272 cm^{-1}) and some alkenes (=C-H at 3040 cm^{-1}, C=C at 1625 cm^{-1} and=C-H at 1000–885 cm^{-1}) is also expected.

The QMS analysis also confirms these results. As it is seen, Fig. 7, on the QMS spectra the presence of the following *m/z* ions: 44 (CO_2), 28 (CO), 18, 17, 16 (H_2O), 69, 82, 41, 87, 67, 55, 54, 39, 83, 81 (cyclohexyl methacrylate), 41, 39, 42, 27, 40, 38, 37, 26, 15, 14 (propene), 56, 84, 41, 55, 69, 39, 42, 27, 43, 54 (cyclohexane), 29, 46, 45, 28, 17, 44, 16, 12, 13, 30 (formic acid), 57, 58, 65, 67, 68, 69, 70, 77, 79, 81, 82, 91 (citronellyl methacrylate), 71, 68, 41, 69, 43, 55, 81, 56, 57, 67 (citronellol), 41, 69, 55, 95, 43, 56, 67, 29, 39, 27 (citronellal), 41, 86, 39, 40, 45, 69, 38, 68, 41, 37 (methacrylic acid) is confirmed [59]. The results indicate the formation of the same main decomposition products as compared to the volatiles emitted in helium. This leads to the conclusion that in both atmospheres the decomposition of the copolymers occurs according to radical mechanism including many simultaneous radical reactions such as breaking of the C–C and C-O bonds in the side and main chains. The presence of oxygen does not significantly

Table 7 The TG-DTG data for copolymers (synthetic air atmosphere))

Polymer name	$T_{5\%}$ /°C	T_{max1} /°C	Δm_1 /%	T_{max2} /°C	Δm_2 /%	T_{max3} /°C	Δm_3 /%	*r*m /%
Copolymer 1	186	349	60.7	405	33.2	504	6.1	0
Copolymer 2	217	352	67.8	402	26.8	508	5.4	0
Copolymer 3	160	165/350	60.7	399	34.1	496	5.2	0
PCitM*	241	292/392	93.7	505	6.3	–	–	0
PCM	205	240/292.5	100	–	–	–	–	0

*As cited in Ref [50]

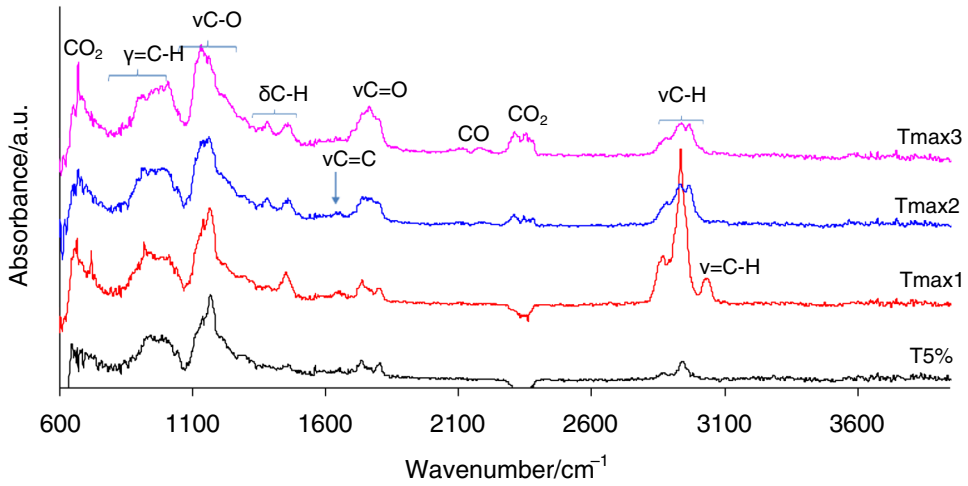

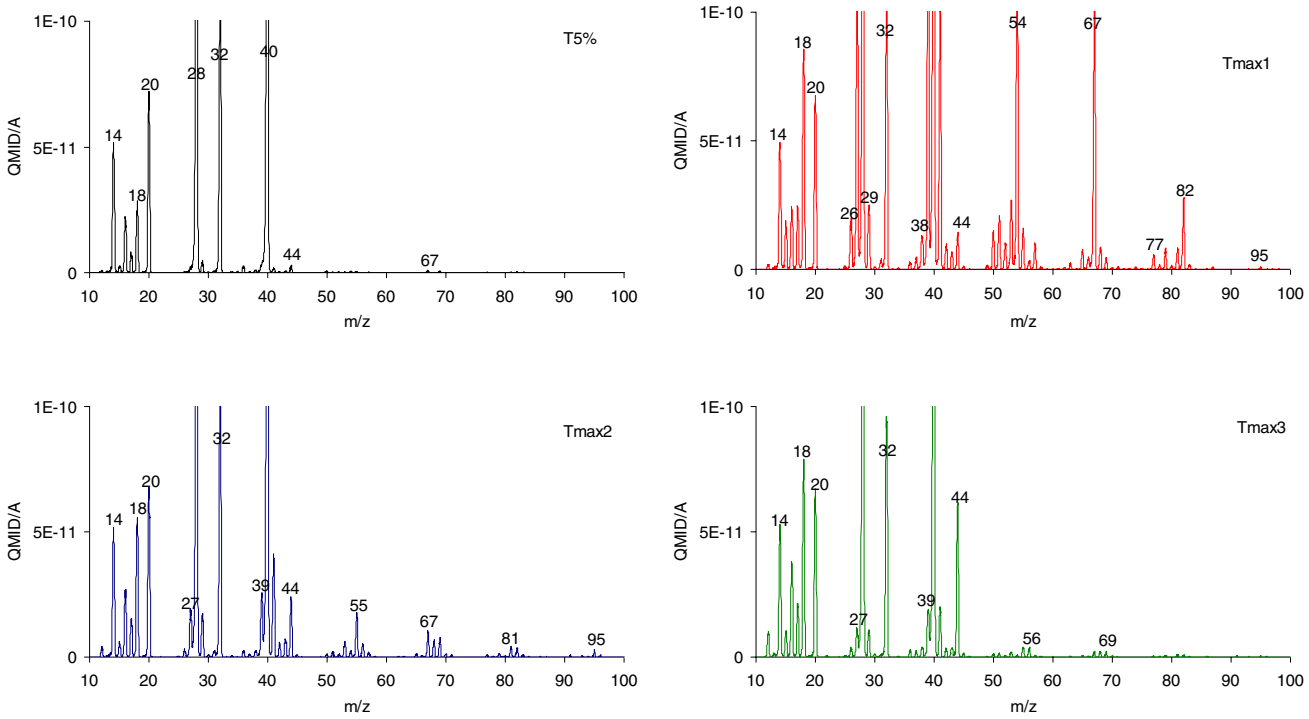

Fig. 6 The FTIR spectra of the emitted volatiles for copolymers in synthetic air (copolymer 2)

Fig. 7 The *m/z* ions of the emitted volatiles at the characteristic temperatures in synthetic air (copolymer 2)

affect the type of the products, but it reduces the activation energy of the decomposition process, which is manifested by a lower thermal resistance of the copolymers in this atmosphere.

Conclusions

The carried DSC and TG/FTIR/QMS analyses confirmed that the thermal properties of novel, more environmentally friendly, high solvent and chemical resistant UV-polymerized materials were directly depended on their composition. It was found that as the content of citronellyl methacrylate in the composition increased, the glass transition temperature and the thermal resistance of the copolymers decreased. By selecting the optimal composition of the copolymers: 50 mass% of citronellyl methacrylate and 50 mass% of cyclohexyl methacrylate, it was possible to obtain polymeric materials with optimal and the best thermal properties, namely a thermal stability above 213 ˚C in inert and oxidizing atmospheres and a glass transition temperature within 37 ˚C.

The simultaneous TG/DTG/FTIR/QMS analysis proved the emission of the same volatiles such as citronellyl methacrylate, cyclohexyl methacrylate, propene, cyclohexane, formic acid, citronellol, citronellal and methacrylic acid in inert and oxidizing conditions. It indicated the same radical decomposition mechanism including the symmetric cleavage of C–C and C-O bonds during the heating of the materials.

Supplementary Information The online version contains supplementary material available at https://doi.org/10.1007/s10973-023-12655-7.

Author contribution M.W. wrote the whole paper and did related data analysis. K.M., P.J. and M.R. performed sample preparation and analysis. All authors read and contributed to the manuscript.

Declarations

Conflict of interest The authors declare that they have no known competing financial interests or personal relationships that could have appeared to influence the work reported in this paper.

References

1. García-Valdez O, Champagne P, Cunningham MF. Graft modification of natural polysaccharides via reversible deactivation radical polymerization. Prog Polym Sci. 2018;76:151–73.
2. Jaymand M. Chemically modified natural polymer-based theranostic nanomedicines: Are they the golden gate toward a *de Novo* clinical approach against anticancer? CS Biomater Sci Eng. 2020;6:134–66.
3. Roy D, Semsarilar M, Guthrie JT, Perrier S. Cellulose modification by polymer grafting: a review. Chem Soc Rev. 2009;38:2046–64.
4. Qiao KL, Zhang XG. Chemical modification of wheat protein-based natural polymers: grafting and cross-linking reactions with poly(ethylene oxide) diglycidyl ether and ethyl diamine. Biomacromol. 2007;8:2909–15.
5. Bhosale RR, Gangadharappa HV, Moin A, Gowda DV, Osmani RAM. Grafting technique with special emphasis on natural gums: applications and perspectives in drug delivery. J Nat Prod. 2015;5:124–9.
6. Martinelli A, Giannini L, Branduardi P. Enzymatic modification of cellulose to unlock its exploitation in advanced materials. ChemBioChem. 2021;22:974–81.
7. Malcom PS. Polymer Chemistry: An Introduction. 3rd ed. NY: Oxford University Press; 1998.
8. Henri L. Thermohygroelastic properties of polymethylmethacrylate. Netherlands; 2007.
9. Musil M, Michalek J, Abbrent S, Kovarova J, Pradny M, Doubkova L, Vondrak J, Sedlarikova M. New type of gel polyelectrolytes based on selected methacrylates and their characteristics. Part I. Copolymers with (3-(trimethoxysilyl)propyl methacrylate). Electrochim Acta 2015;155:183–195.
10. Gibson I, Rosen DW, Stucker B. Photopolymerization processes. Additive manufacturing technologies, rapid prototyping to direct digital manufacturing. Springer-Verlag US:Boston MA; 2010.
11. Liu R, Zhu J, Luo J, Liu X. Synthesis and application of novel UV-curable hyperbranched methacrylates from renewable natural tannic acid. Prog Org Coat. 2014;77:30–7.
12. Grumezescu AM. Organic materials as smart nanocarriers for drug delivery. Elsevier Inc.; 2018.
13. Stanzione JF, Sadler JM, La Scala JJ, Reno KH, Wool RP. Vanillin-based resin for use in composite applications. Green Chem. 2012;14:2346–52.
14. Zhang C, Madbouly SA, Kessler MR. Renewable polymers prepared from vanillin and its derivatives. Chem Phys. 2015;216:1816–22.
15. Stanzione JF, Sadler JM, La Scala JJ, Wool RP. Lignin model compounds as bio-based reactive diluents for liquid molding resins. Chemsuschem. 2012;5:1291–7.
16. Molina-Gutiérrez S, Manseri A, Ladmiral V, Bongiovanni R, Caillol S, Lacroix-Desmazes P. Eugenol: a promising building block for synthesis of radically polymerizable monomers. Macromol Chem Phys. 2019;220:1–10.
17. Sainz MF, Souto JA, Regentova D, Johansson MKG, Timhagen ST, Irvine DJ, Buijsen P, Koning CE, Stockman RA, Howdle SM. A facile and green route to terpene derived acrylate and methacrylate monomers and simple free radical polymerisation to yield new renewable polymers and coatings. Polym Chem. 2016;7:2882–7.
18. Zweifel G, Brown HC. Hydroboration of terpenes. II. The hydroboration of α- and β-pinene-the absolute configuration of the dialkylborane from the hydroboration of α-pinene. J Am Chem Soc. 1964;86:393–397.
19. Cravero RM, González-Sierra M, Labadie GR. Convergent approaches to saudin intermediates. Helv Chim Acta. 2003;86:2741–53.
20. Elamparuthi E, Fellay C, Neuburger M, Gademann K. Total synthesis of cyrneine A. Angew Chemie Int Ed. 2012;52:4071–3.
21. Kei Matsuzaki KK, Hosonuma K, Kanai T. Copolymerization of (−)- and (±)-menthyl acrylates. Die Makromol Chemie. 1975;176:2853–60.
22. Lima MS, Costa CSMF, Coelho JFJ, Fonseca AC, Serra AC. A simple strategy toward the substitution of styrene by sobrerol-based monomers in unsaturated polyester resins. Green Chem. 2018;20:4880–90.
23. Noppalit S, Simula A, Ballard N, Callies X, Asua JM, Billon L. Renewable terpene derivative as a biosourced elastomeric building block in the design of functional acrylic copolymers. Biomacromol. 2019;20:2241–51.
24. Hasegawa S, Azuma M, Takahashi K. Stabilization of enzyme activity during the esterification of lactic acid in hydrophobic ethers and ketones as reaction media that are miscible with lactic acid despite their high hydrophobicity. Enzyme Microb Technol. 2008;43:309–16.
25. Purushothaman M, Krishnan PSG, Nayak SK. Poly(alkyl lactate acrylate)s having tunable hydrophilicity. J Appl Polym Sci. 2015;131:1–11.
26. Mansoori Y, Hemmati S, Eghbali P, Zamanloo MR, Imanzadeh G. Nanocomposite materials based on isosorbide methacrylate/Cloisite 20A. Polym Int. 2013;62:280–8.
27. Gallagher JJ, Hillmyer MA, Reineke TM. Isosorbide-based polymethacrylates ACS Sustain Chem Eng. 2015;3:662–7.

28. Gallagher JJ, Hillmyer MA, Reineke TM. Acrylic triblock copolymers incorporating isosorbide for pressure sensitive adhesives. ACS Sustain Chem Eng. 2016;4:3379–87.
29. Yu DM, Smith DM, Kim H, Rzayev J, Russell TP. Two-step chemical transformation of polystyrene-*block*-poly(solketal acrylate) copolymers for increasing χ. Macromolecules. 2019;52:6458–66.
30. Yu X, Picker MT, Schneider M, Herberg A, Pascual S, Fontaine L, Kuckling D. Synthesis of amphiphilic block copolymers based on SKA by RAFT polymerization. Macromol Chem Phys. 2018;219:1700506.
31. Anastasaki A, Nikolaou V, Simula A, Godfrey J, Li M, Nurumbetov G, Wilson P, Haddleton DM. Expanding the scope of the photoinduced living radical polymerization of acrylates in the presence of $CuBr_2$ and M_e6-tren. Macromolecules. 2014;47:3852–9.
32. Pham PD, Monge S, Lapinte V, Raoul Y, Robin JJ. Glycerol-based co-oligomers by free-radical chain transfer polymerization: Towards reactive polymers bearing acetal and/or carbonate groups with enhanced properties. Eur Polym J. 2017;95:491–502.
33. Zamzow M, Höcker H. Synthesis of polymers with pendant spiro orthoester groups. Chem Phys. 1994;195:2381–400.
34. Ray P, Hughes T, Smith C, Hibbert M, Saito K, Simon GP. Development of bio-acrylic polymers from Cyrene™: transforming a green solvent to a green polymer. Polym Chem. 2019;10:3334–41.
35. Badía A, Movellan J, Barandiaran MJ, Leiza JR. High biobased content latexes for development of sustainable pressure sensitive adhesives. Ind Eng Chem Res. 2018;57:14509–16.
36. Badía A, Santos JI, Agirre A, Barandiaran MJ, Leiza JR. UV-tunable biobased pressure-sensitive adhesives containing piperonyl methacrylate. ACS Sustain Chem Eng. 2019;7:19122–30.
37. Campanella A, La Scala JJ, Wool RP. The use of acrylated fatty acid methyl esters as styrene replacements in triglyceride-based thermosetting polymers. Polym Eng Sci. 2009;49:2384–92.
38. Ladmiral V, Jeannin R, Fernandes Lizarazu K, Lai-Kee-Him J, Bron P, Lacroix-Desmazes P, Caillol S. Aromatic biobased polymer latex from cardanol. Eur Polym J. 2017;3:785–94.
39. Worzakowska M. Chemical modification of potato starch by graft copolymerization with citronellyl methacrylate. J Polym Environm. 2018;26:1613–24.
40. Worzakowska M. The preparation, physicochemical and thermal properties of the high moisture, solvent and chemical resistant starch-g-poly(geranyl methacrylate) copolymers. J Therm Anal Calorim. 2020;140:189–98.
41. Worzakowska M. Novel starch-g-copolymers obtained using acrylate monomers prepared from two geometric isomers of terpene alcohol. Eur Polym J. 2019;110:265–75.
42. Tuncel K, Ecevit K, Kenesci K, Piskin E. Nonswellable and swellable ethylene glycol dimethacrylate-acrylic acid copolymer microspheres. J Polym Sci A Polym Chem. 1996;34:45–55.
43. Worzakowska M. Starch-g-PCHMA copolymers – preparation and properties. J Therm Anal Calorim. 2022;147:1225–35.
44. Chen J, Garcia ES, Zimmerman SC. Intramolecularly crosslinked polymers: from structure to function with applications as artificial antibodies and artificial enzymes. Acc Chem Res. 2020;53:1244–56.
45. Lederer A, Burchars W. Degree of branching in hyperbranched polymers: macromolecules in between deterministic linear chains and dendrimer structures. Cambridge: Royal Society of Chemistry; 2015.
46. Viville P, Schappacher M, Lazzaroni R, Deffieux A. Highly-branched polymers: from comb to dendritic architectures. Synthetic routes and morphological study in solution and in thin films. Soft-matter characterization. In. Borsali R, Pecora R, editors. Springer; 2008.
47. Abedin MJ, Liepold L, Suci P, Young M, Douglas T. Synthesis of a crosslinked branched polymer network in the interior of a protein cage. J Am Chem Soc. 2009;131:4346–54.
48. Worzakowska M. TG/DSC/FTIR/QMS analysis of environmentally friendly poly(citronellyl methacrylate)-co-poly(benzyl methacrylate) copolymers. J Mater Sci. 2023;58:2005–24.
49. Worzakowska M. TG-FTIR-QMS analysis of more environmentally friendly poly(geranyl methacrylate)-co-poly(cyclohexyl methacrylate) copolymers. Polym Degrad Stabil. 2022;206:110196.
50. Worzakowska M. High chemical and solvent resistant, branched terpene methacrylate polymers-Preparation, thermal properties, and decomposition mechanism. Polym Adv Technol. 2018;29:1414–25.
51. NIST Chemistry Webbook, NIST Standard Reference Data, 2011, http://webbook.nist.gov
52. Parparita E, Nistor MT, Popescu MC, Vasile C. TG/FTIR/MS study on thermal decomposition of polypropylene/biomass composites. Polym Degrad Stabil. 2014;109:13–20.
53. Xu J, Liu C, Qu H, Ma H, Jiao Y, Xie J. Investigation on the thermal degradation of flexible poly(vinyl chloride) filled with ferrites as flame retardant and smoke suppressant using TGA-FTIR and TGA-MS. Polym Degrad Stabil. 2013;98:1506–14.
54. AlAbbad M, Gautam R, Romero EG, Saxena S, Barradah E, Chatakonda O, Kloosterman JW, Middaugh J, D'Agostini MD, Sarathy M. TG-DSC and TG-FTIR analysis of heavy fuel oil and vacuum residual oil pyrolysis and combustion: characterization, kinetics, and evolved gas analysis. J Therm Anal Calorim. 2023;148:1875–98.
55. Zhang D, Yang R, Qin Z, Zang W. Study on the thermal behaviors of polyhedral oligomeric octaphenylsilsesquioxane (OPS). J Therm Anal Calorim. 2023;148:2345–55.
56. Hu WJ, Li YM, Li YR, Wang DY. Highly efficient intumescent flame retardant of dopamine-modified ammonium polyphosphate for the thermoplastic polyurethane elastomer. J Therm Anal Calorim. 2023;148:1841–51.
57. Wang Y, Liu SH. Investigation on the thermal hazard and decomposition behaviors of *tert*-butyl (2-ethylhexyl) monoperoxy carbonate via STA, DSC, and FTIR. J Therm Anal Calorim. 2023;148:4969–76.
58. Zhang D, Liu M, Wen H, Deng J, Wang W, Shu CM. Use of coupled TG-FTIR and Py-GC/MS to study combustion characteristics of conveyor belts in coal mines. J Therm Anal Calorim. 2023;148:4779–89.
59. The NIST mass spectral search program for the NIST/EPA/NIH mass spectral library, version 2.0f, build Jan 25 2008 software by Stein S, Mirokhin Y, Tchekhovskoi D, Mallard G, data evolution by Mikaia A, Zaikin V, Little J, Zhu D, White W, Sparkman D.
60. Simič R, Mandal J, Zhang K, Spencer ND. Oxygen inhibition of free-radical polymerization is the dominant mechanism behind the "mold effect" on hydrogels. Soft Matter. 2021;17:6394–403.
61. Gauthier MA, Stangel I, Ellis TH, Zhu XX. Oxygen inhibition in dental resins. J Dent Res. 2005;84:725–9.
62. Zhao JR, Xiao Y, Zhong KQ, Li QW, Zhai XW. Effects of oxygen concentration and heating rate on coal spontaneous combustion characteristics. J Therm Anal Calorim. 2023;148:4949–58.